

Supplementary Information

Self-cycled photocatalytic Fenton system and rapid degradation of organic pollutants over magnetic 3D MnS nanosheet/iron-nickel foam

Xiaoqian Ma^{a,b}, Yu Liu^{a,b}, Yi Zhao^{a,b}, Xiaohong Chen^a, Junyang Leng^{a,b}, Anlong Zhang^{a,b}, Daomei Chen^{a,b}, Kai Xiong^{a,b}, Jiaqiang Wang^{a,b*}

^a School of Chemical Sciences & Technology, School of Materials and Energy, Institute of International Rivers and Eco-security, Yunnan Province Engineering Research Center of Photocatalytic Treatment of Industrial Wastewater, National Center for International Research on Photoelectric and Energy Materials, Yunnan University, Kunming 650091, P. R. China

^b Institute of Frontier Technologies in Water Treatment Co., Ltd., Kunming, 650503, P. R. China

**Corresponding author. Tel.: +86-871-65031567.*

Fax: +86-871-65031567.

E-mail address: jqwang@ynu.edu.cn (J. Wang)

H₂O₂ detection methods

A phosphate buffer was prepared by dissolving 2.8756 g K₂HPO₄·3H₂O and 11.935 g KH₂PO₄ in 200 mL deionized water. Then prepared N, N-diethyl-1,4-phenylenediamine sulfate (DPD, 97%, Aldrich) and peroxidase (POD, horseradish, Aldrich) stock solutions. (Dissolve 0.1 g DPD in 10 ml 0.05 M H₂SO₄ solution and 10 mg POD in 10 ml deionized water.) During the experiment, take 2.5ml sample solution into a quartz tube each time, added 0.4 ml phosphate buffer and 50 μL POD solution in sequence. Liter and 50 microliters of DPD solution, mix well. Useing UV-2600 (Shanghai Tianmei Scientific Instrument Co., Ltd.) to measure absorbance at 552 nm. Calibrate the H₂O₂ concentration by diluting a 30% H₂O₂ stock solution.

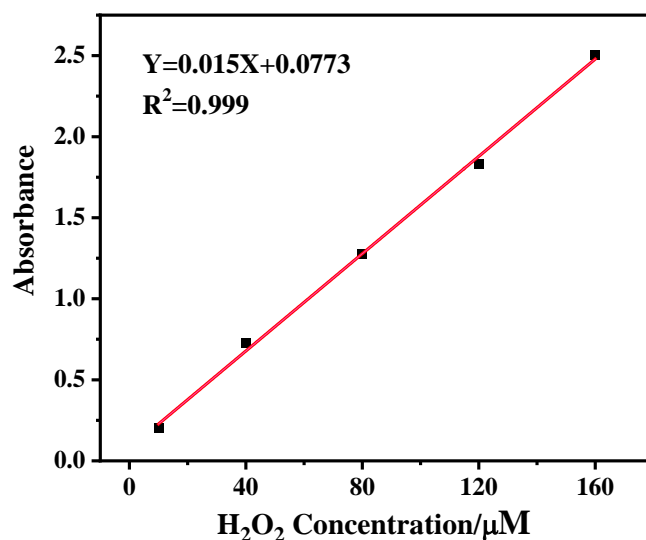


Fig. S1. Standard curve for H₂O₂.

Fe(II) detection methods

The concentration of Fe(II) were probed by the 1,10-phenanthroline monohydrate based on the standard plot of FeSO₄. Then, approximately 1.0 mL of the suspension was collected from the reaction solution at each given time intervals, which was centrifugated to obtain clear solution. The clear solution was mixed with 1,10-phenanthroline monohydrate (1 mg/mL, 1.0 mL). After that, the absorbance of the mixture was investigated by UV-vis spectroscopy (UV-mini 1280) to evaluate the corresponding concentration of Fe²⁺.

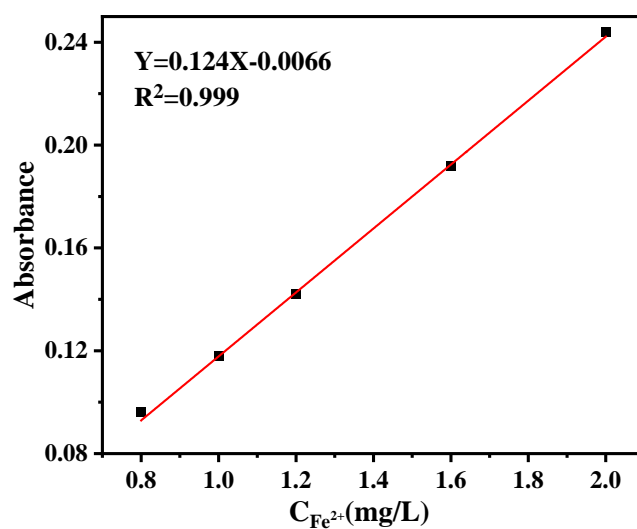


Fig. S2. Standard curve for Fe²⁺.

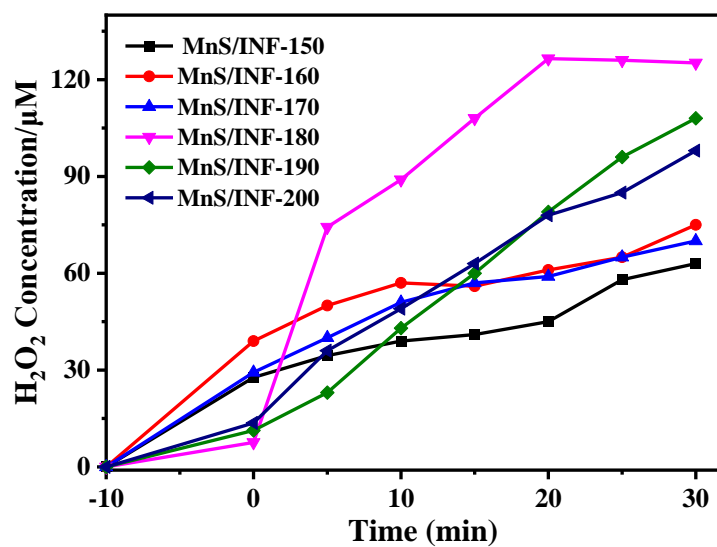


Fig. S3. Photocatalytic H₂O₂ production of MnS/INF-prepared at different temperature within 30 min.

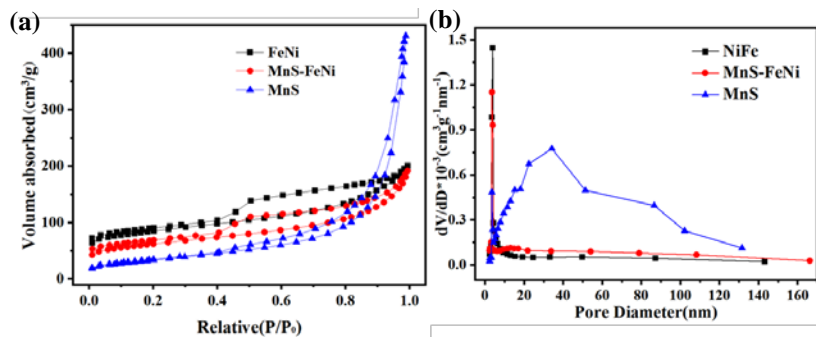


Fig. S4. BET curves and (h) the BJH pore distribution of samples

Table. S1 The specific surface area and pore structure data of MnS/INF

Catalyst	Surface area (m ² /g)	Pore volume (cm ³ /g)	Pore size (nm)
INF	1.67	0.0047	11.4
MnS	2.79	0.031	4.6
MnS/INF	10.9	0.028	9.9

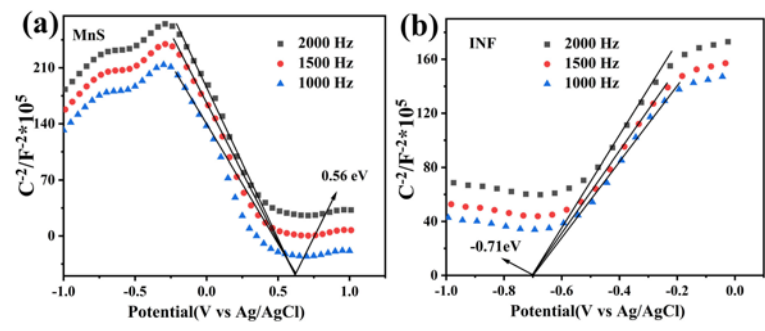


Fig. S5. Mott-schottky of (a) INF, (b)MnS and (c) MnS/INF samples.

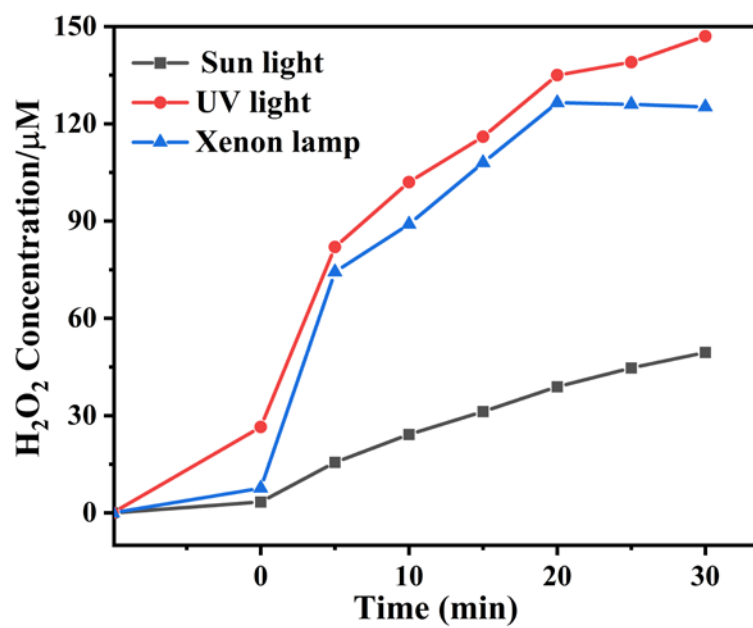


Fig. S6. Photocatalytic H₂O₂ production under different light sources within 30 min.

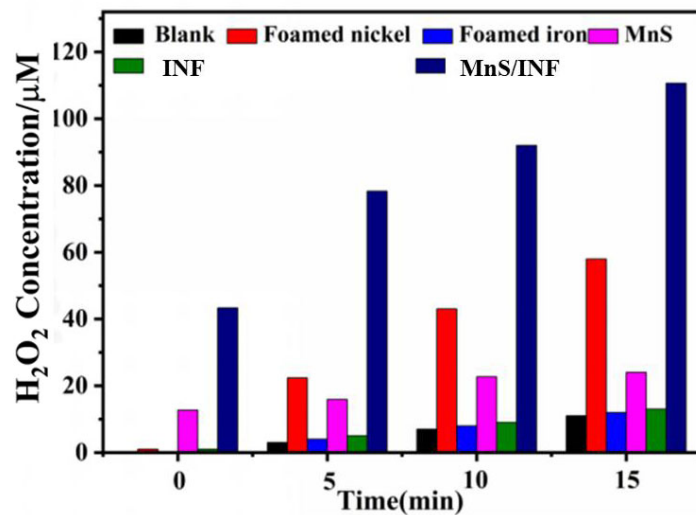


Fig. S7. Comparison of photocatalytic H₂O₂ production between Foamed nickel, Foamed iron, MnS, Foamed iron-nickel and MnS/INF at 15min.

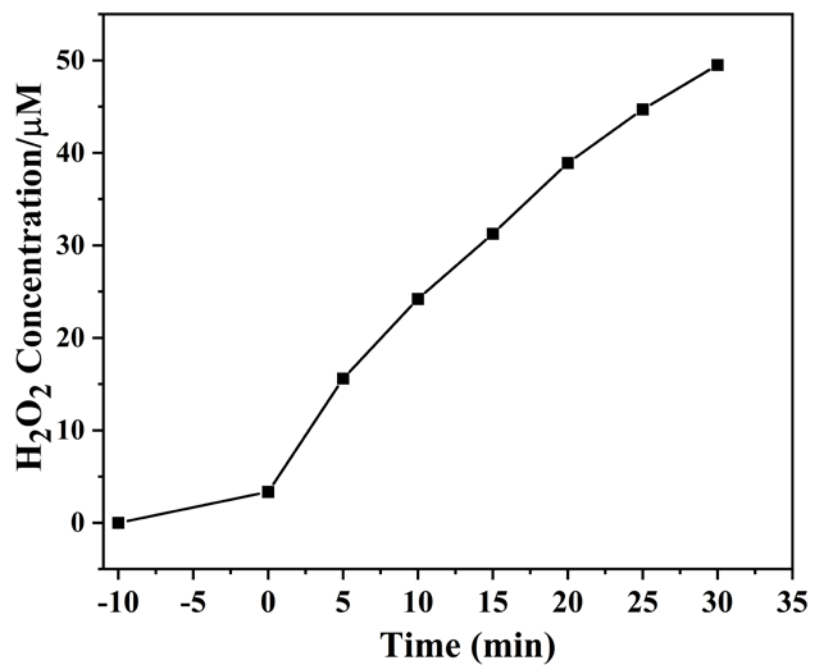


Fig. S8. The self-decomposition rate of H₂O₂.

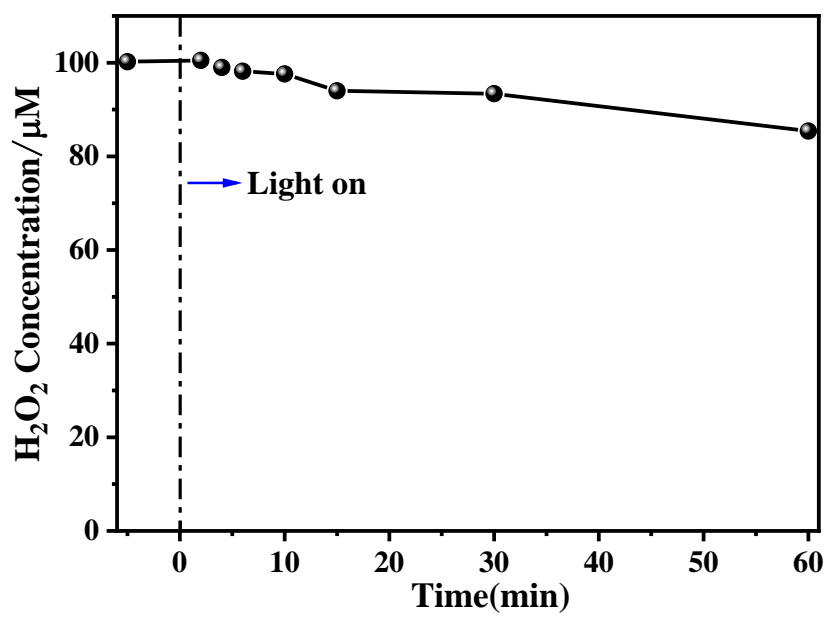


Fig. S9. The self-decomposition rate of H_2O_2 .

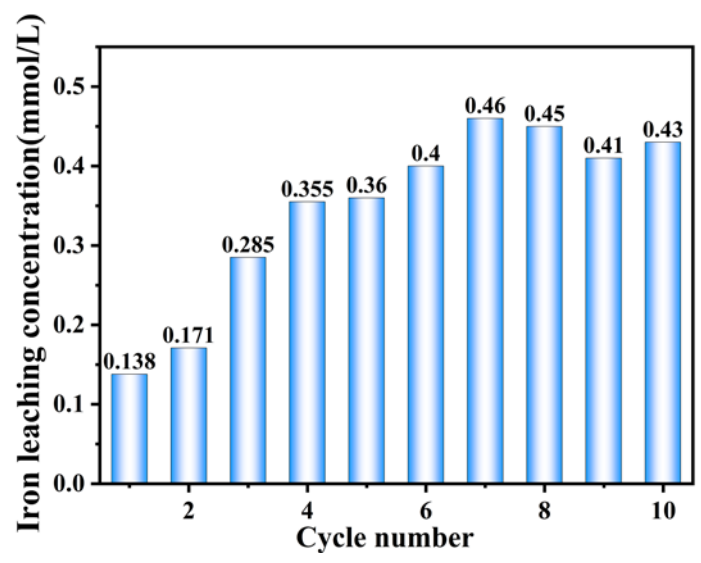


Fig. S10. Variation of iron ion concentration with cycle times.

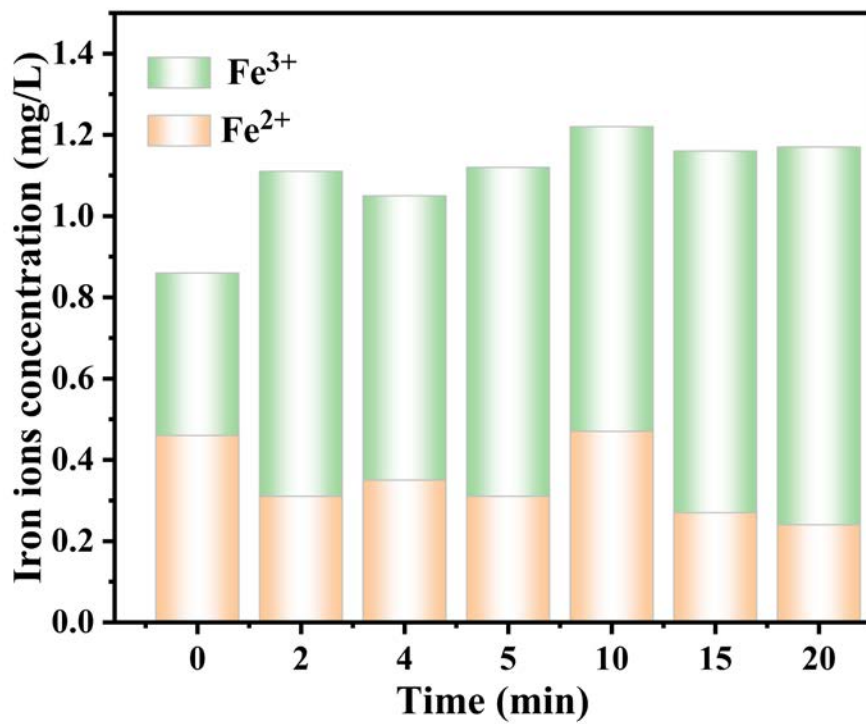


Fig. S11. Variation of Fe²⁺ and Fe³⁺ concentration with times.

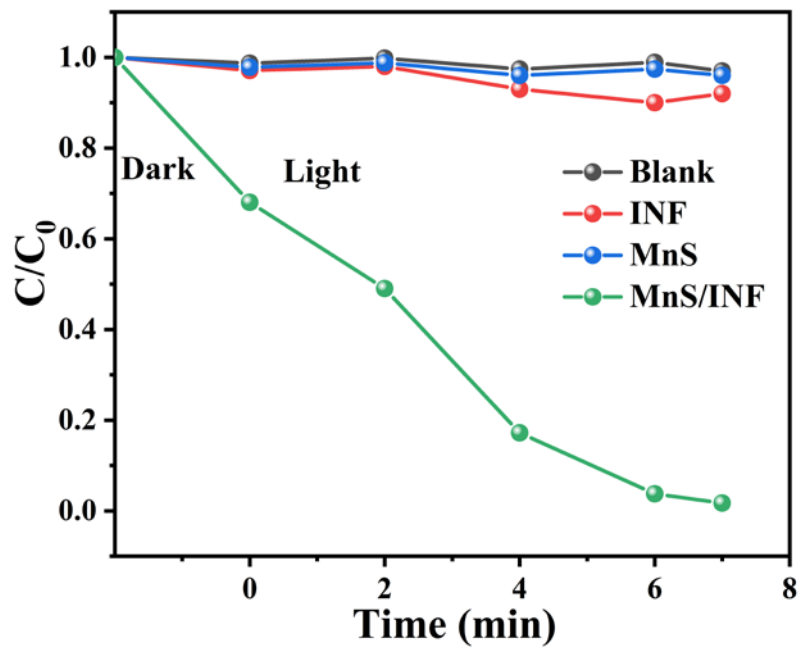


Fig. S12. Degradation kinetic curves of RhB by INF, MnS, and MnS/INF.

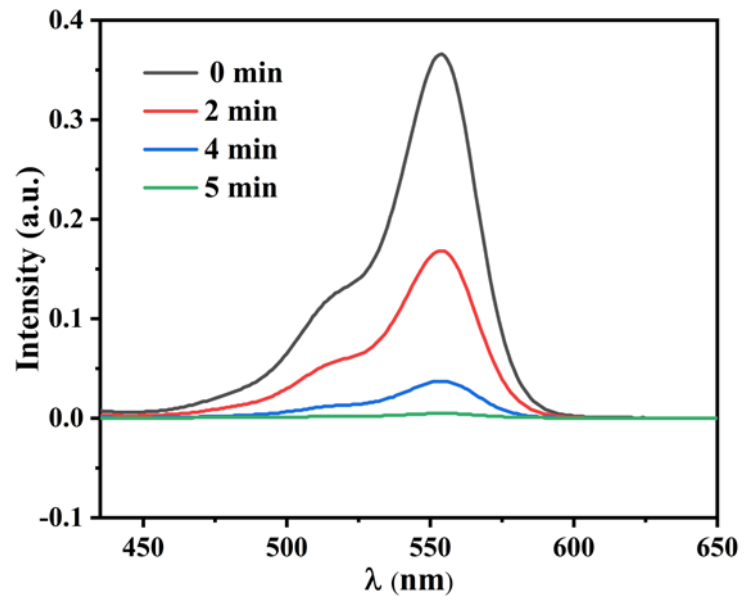


Fig. S13. Variation of the UV-Vis spectrum of RhB with time over MnS/INF.

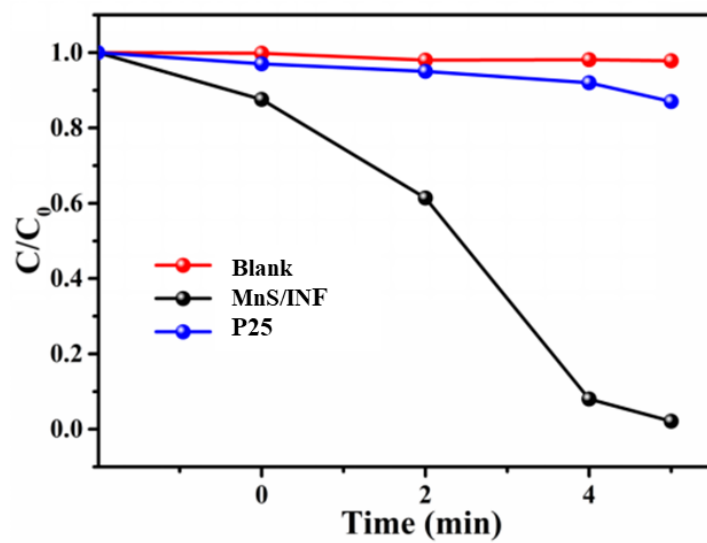


Fig. S14. Degradation kinetic curves of RhB by blank, MnS/INF and P25.

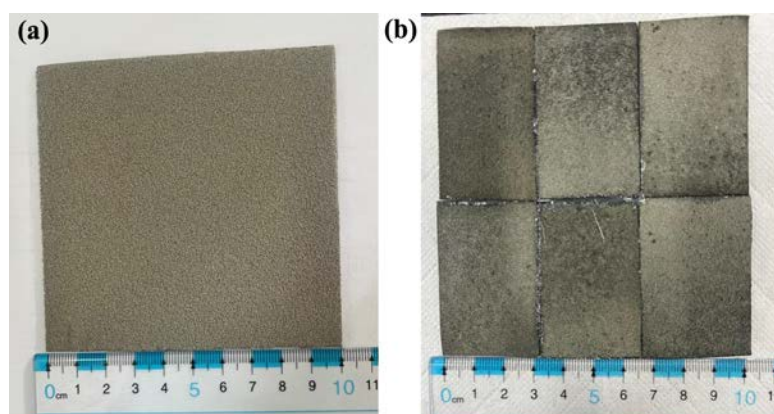


Fig. S15. (a) Photographs of 100 cm² iron nickel foamed and (b) The spliced MnS/INF 100 cm² after hydrothermal synthesis.

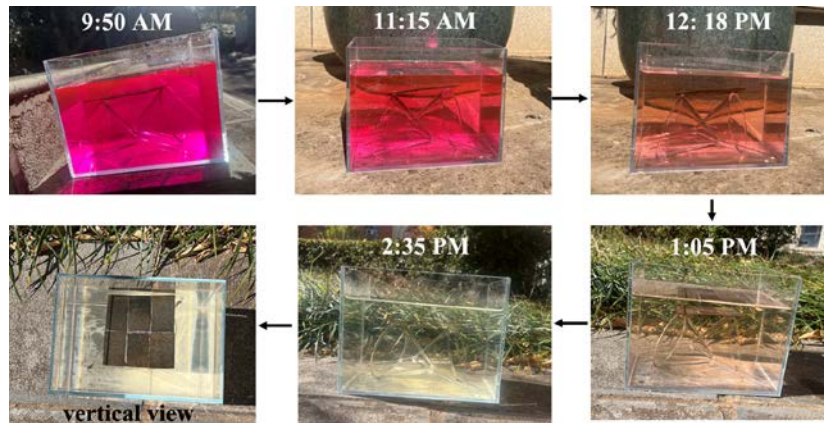


Fig. S16. Optical image of the degradation process of 4.5L RhB solution (5 mg/L) with 100 cm² catalyst under 4.75 h, with input of only oxygen (oxygen is given every 30 minutes) and sunlight.

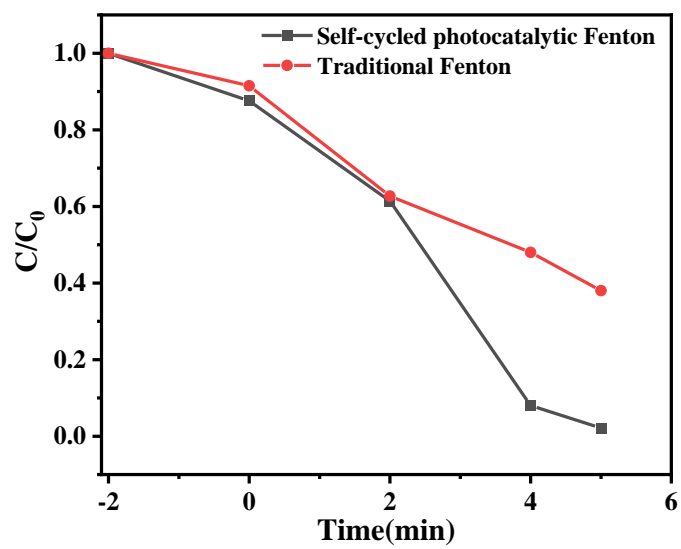


Fig. S17. Degradation kinetic curves of RhB by self-cycled photocatalytic Fenton and traditional Fenton within 5 min.

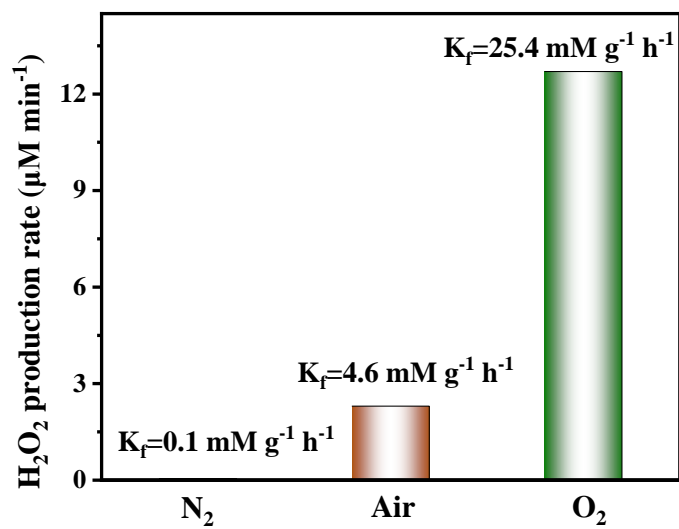


Fig. S18. Photocatalytic production of H₂O₂ by MnS/INF under different atmosphere conditions (condition: 30 mg catalyst, 50 mL H₂O, LED light ($\lambda > 420$ nm)).

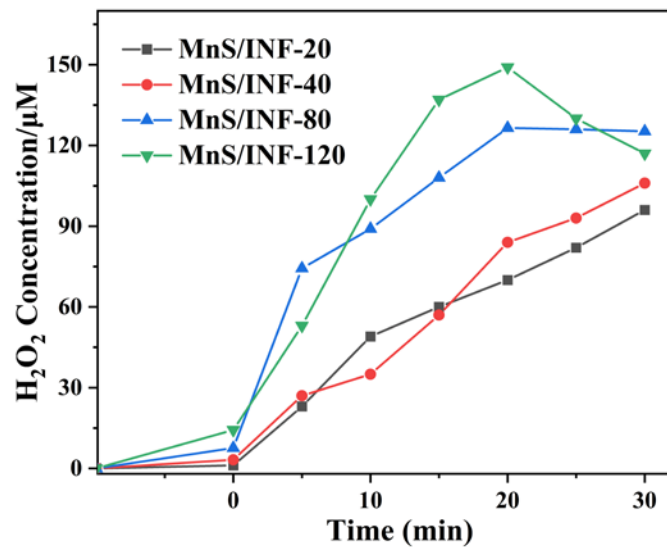


Fig. S19. Time course for the photocatalytic H₂O₂ production by MnS/INF-20, MnS/INF-40, MnS/INF-80 and MnS/INF-120.

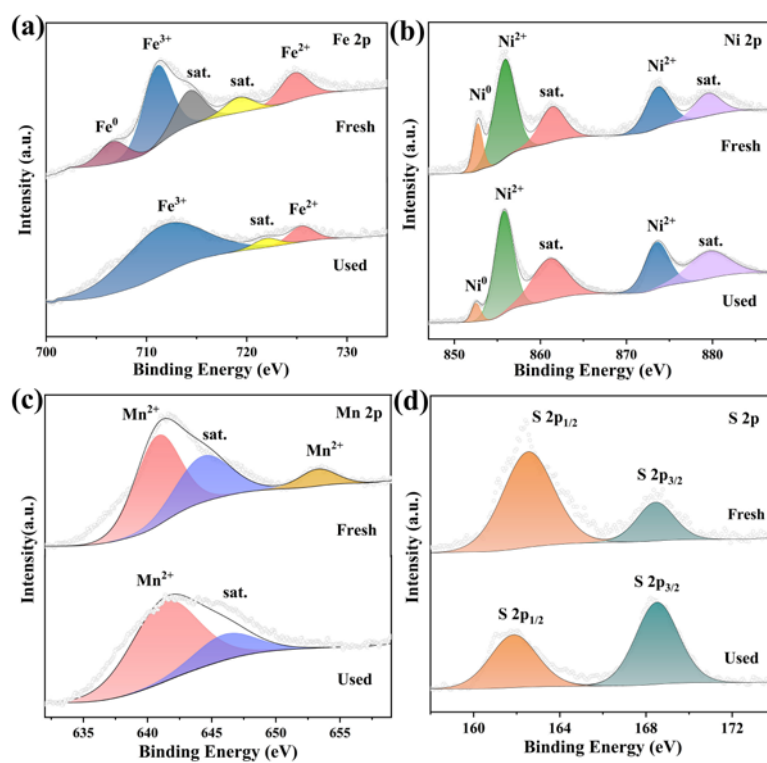


Fig. S20. XPS spectra of the MnS/INF before reaction and after photocatalytic reaction. High resolution XPS spectra of (a) Fe 2p, (b) Ni 2p, (c) Mn 2p, (d) S 2p.

Table S2 The amount of iron sludge produced by treating hospital wastewater with MnS/IN and traditional Fenton technology.

		The concentration of iron ion after photocatalytic reaction 1h		The concentration of iron ion after photocatalytic reaction 2h	
MnS/INF (30mg)	pH=6	0.98 mg/L		1.56 mg/L	
Traditional Fenton technology Fe ²⁺ (30mg)	pH=3	74.6 mg/L		77 mg/L	
	pH=6	100 mg/L		139 mg/L	

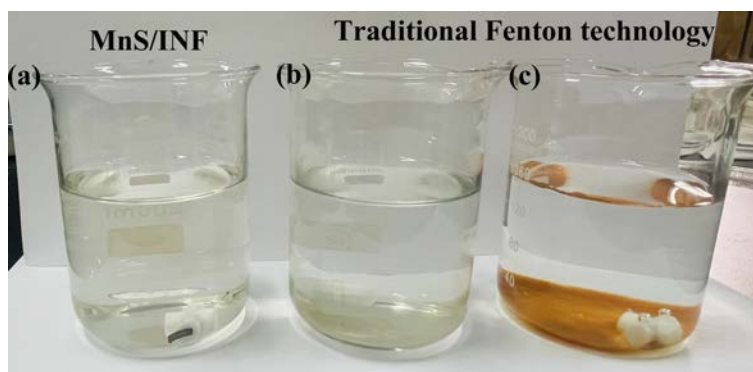


Fig. S21. Photo of iron sludge produced by treating hospital wastewater with MnS/INF(a) and traditional Fenton technology (b,c).